The Multiplet Cavity: A Buncher for Broad-Bandwidth Klystron Amplifiers

Alan Bromborsky, *Member, IEEE*

***Abstract*— The bandwidth of a klystron output cavity scales (approximately) as $\wp^{0.8}P^{0.2}$, where $\wp$ is the beam perveance and P is the beam power [1], [2]. For high-perveance ($\wp >$ 10 μpervs) high-power ($P >$ 10 kW) electron beams, it is relatively straightforward to design a broad-band output cavity. However, the design of the input cavity of the broad-band klystron is in some ways more difficult. The purpose of the input cavity is to produce a velocity-modulated electron beam with a frequency-dependent modulation amplitude that will optimize the bandwidth of the entire klystron system, while providing a magnitude of velocity modulation large enough to minimize the length of the klystron. This paper shows how a multiplet (multiple cavity) buncher cavity can be designed to provide broad-band (>20%) operation while keeping short the drift section length of the klystron.**

NOMENCLATURE

If l is the mode index and k is the cavity index, we can define the following quantities for future use (see Figs. 1 and 2 for $V_{\rm gen}(t)$ and $Z_{\rm gen}$):

c	Speed of light in vacuum (m/s).
Z_0	Impedance of free space (Ω).
ϵ_0	Permittivity of free space (F/m).
$V_{\rm beam}$	Static beam accelerating voltage (V).
$Z_{\rm beam}$	Static beam impedance (Ω).
$V_{\rm gen}(t)$	Time-dependent generator voltage (V).
$Z_{\rm gen}$	Generator impedance (Ω).
$c_{l,k}(t)$	lth mode vector potential amplitude in the kth cavity.
$\omega_{l,k}$	lth mode cavity resonant frequency (rad/s, possibly complex) in the kth cavity.
$\mathcal{E}_{l,k}(\boldsymbol{x}_k)$	Spatial distribution of lth electric field eigenmode (V/m) in the kth cavity.
Ω_k	Spatial region of kth cavity interior.
$s_{k\,\rm loop}$	Path of drive loop in the kth cavity.
$V_{l,k\,\rm loop}$	Path integral of $\mathcal{E}_{l,k}(\boldsymbol{x}_k)$ over the section of the drive loop in the kth cavity (V).
$\boldsymbol{E}_{l,k}(\boldsymbol{x},t)$	Electric field (V/m) of lth driven mode in the kth cavity.
$\boldsymbol{J}_{k\,\rm loop}(\boldsymbol{x}_k,t)$	Time-dependent drive loop current density in the kth buncher gap (A/m^2).
$\boldsymbol{J}_k(\boldsymbol{x}_k,t)$	Time-dependent electron beam current density in the kth buncher gap (A/m^2).
D_k	Length of buncher gap in kth cavity (m).
$V_{l,k\,\rm gap}$	Path integral of $\mathcal{E}_{l,k}(\boldsymbol{x}_k)$ over buncher gap in kth cavity (V).
$G_{l,k}$	Gap gain, the ratio $V_{l,k\,\rm gap}/V_{l,k\,\rm loop}$.
$V_{l,k}$	The voltage induced across the buncher gap by the lth driven mode in the kth cavity (V).
$J_{z_k}(z_k)$	The z-component of the current density in the kth buncher gap (A/m^2).
z_k	The axial z distance measured from the input of the kth buncher gap (m).

Manuscript received September 1, 1995; revised February 1, 1996. This work was performed for the United States Army Research Laboratory, Adelphi, MD.

The author is with the United States Army Research Laboratory (AMSRL-WT-NH), Adelphi, MD 20783-1197 USA (e-mail: brombo@lamp0.arl.army.mil).

Publisher Item Identifier S 0093-3813(96)04685-1.

I. INTRODUCTION

ONE POSSIBLE bandwidth-enhancing modification of a standard klystron buncher cavity is the multiplet configuration, where N cavities are driven by the same generator (Fig. 1 is an example of a doublet cavity, $N = 2$), but where the bunching gaps are concatenated, so that the modulated beam emerging from the buncher gap of cavity k is input to the buncher gap of cavity $k + 1$. By having N cavities with different resonant frequencies and different voltage gains (to be defined later), we have many more degrees of freedom to tailor the velocity modulation of the buncher cavity as a function of the drive frequency, ω. Note that this method is related to that used in the clustered-cavity™ klystron [3], in which the idler cavities are of multiplet form. Since one of the major objectives of our klystron design analysis is to maximize the bandwidth while minimizing the size of the device, we will try to avoid the use of idler cavities if at all possible, while maintaining broad bandwidth operation.

II. MULTIPLET BUNCHER CAVITY ANALYSIS

The analysis of the multiplet buncher cavity consists of two parts, one electromagnetic and one electronic. The electromagnetic parts of the system are the electric fields in the buncher cavity due to the current distributions of the electron beam and the drive loop (see Fig. 1), and the effects of a realistic generator model (see Fig. 2) upon this field. The method used to calculate the cavity field is modal expansion of the vector potential. In this method the vector potential field, $\boldsymbol{A}_k(\boldsymbol{x}_k,t)$, (throughout this paper the index k denotes quantities specific to the kth cavity of the multiplet) driven by the beam and loop currents, is expanded in terms of the empty cavity eigenmodes, $\mathcal{A}_{l,k}(\boldsymbol{x}_k)$, with all mode time variation included in the mode

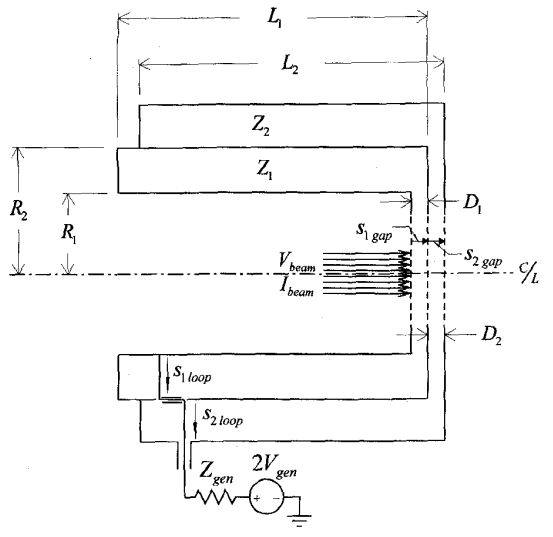

Fig. 1. Doublet buncher cavity.

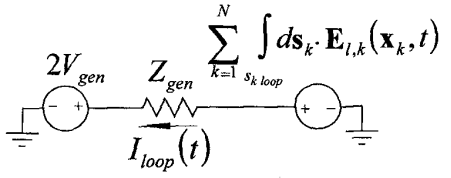

Fig. 2. Thevinin equivalent circuit for drive loop.

coefficient, $c_{l,k}(t)$, so that

$$\boldsymbol{A}_k(\boldsymbol{x}_k, t) = \sum_l c_{l,k}(t)\mathcal{A}_{l,k}(\boldsymbol{x}_k). \tag{1}$$

An integral representation for the gap voltage due to excitation of the lth mode of the kth cavity is derived from the driven mode equation for the vector potential, with parameters that depend upon the cavity geometry, generator source impedance and voltage, and the electron beam current and voltage. The electronic parts of the system are the electron beam velocity and current fields. The method used to calculate these fields is to model the electron beam as a one-dimensional (1-D) fluid. This model gives a system of coupled partial differential equations in time and one space variable that are converted to a system of ordinary differential equations in space (1-D) and are driven by the axial electric field calculated in the electromagnetic part of the analysis. Taken altogether, the electromagnetic and electronic analyses of the multiplet cavity yield a system (three equations for each cavity) of coupled nonlinear integro-differential equations to be solved.

A. Driven Mode Equations

For a multiplet system (see Fig. 1 for a doublet system) the vector potential mode amplitude, $c_{l,k}(t)$, of the lth mode of the kth cavity in the multiplet, that is excited by the combination of a drive loop current density, $\boldsymbol{J}_{k\,\mathrm{loop}}(\boldsymbol{x}_k, t)$, and an electron beam current density, $\boldsymbol{J}_k(\boldsymbol{x}_k, t)$, is a solution to [2]

$$\ddot{c}_{l,k}(t) + \omega_{l,k}^2 c_{l,k}(t) = -\frac{i\omega_{l,k}}{\epsilon_0 \int_{\Omega_k} dV |\mathcal{E}_{l,k}(\boldsymbol{x}_k)|^2} \cdot \int_{\Omega_k} dV \mathcal{E}_{l,k}^*(\boldsymbol{x}_k) \cdot (\boldsymbol{J}_{k\,\mathrm{loop}}(\boldsymbol{x}_k, t) + \boldsymbol{J}_k(\boldsymbol{x}_k, t)). \tag{2}$$

If we assume that the loop current is filamentary, and that the drive loop is short compared to an operating wavelength, then the current in the drive loop will not vary as a function of position along the loop and (2) can be reduced to

$$\ddot{c}_{l,k}(t) + \omega_{l,k}^2 c_{l,k}(t) = -\frac{i\omega_{l,k}}{\epsilon_0 \int_{\Omega_k} dV |\mathcal{E}_{l,k}(\boldsymbol{x}_k)|^2} \cdot \left(V_{l,k\,\mathrm{loop}}^* I_{\mathrm{loop}}(t) + \int_{\Omega_k} dV \mathcal{E}_{l,k}^*(\boldsymbol{x}_k) \bullet \boldsymbol{J}_k(\boldsymbol{x}_k, t) \right). \tag{3}$$

For the remainder of this paper, we will consider only one mode to be excited in any of the N cavities and designate it the lth mode. However, for very broadband systems, more than one mode in each cavity could be excited and would have to be included in the analysis. This complication will be treated in future publications. I_{loop} is calculated by constructing the Thevinin equivalent circuit (see Fig. 2) of the cavity driver giving

$$I_{\mathrm{loop}}(t) = \frac{1}{Z_{\mathrm{gen}}} \cdot \left(\sum_{m=1}^{N} \int_{s_{m\,\mathrm{loop}}} d\boldsymbol{s}_m \bullet \boldsymbol{E}_{l,m}(\boldsymbol{x}_m, t) - 2V_{\mathrm{gen}}(t) \right). \tag{4}$$

Since we are using a modal expansion of the vector potential the cavity electric fields are calculated from the vector potential mode amplitudes by

$$\boldsymbol{E}_{l,k}(\boldsymbol{x}_k, t) = -\frac{i\dot{c}_{l,k}(t)}{\omega_{l,k}} \mathcal{E}_{l,k}(\boldsymbol{x}_k) \tag{5}$$

where the $\mathcal{E}_{l,k}(\boldsymbol{x}_k)$ are electric field eigenmodes. I_{loop} simplifies to

$$I_{\mathrm{loop}}(t) = -\frac{1}{Z_{\mathrm{gen}}} \left(i \sum_{m=1}^{N} \frac{V_{l,m\,\mathrm{loop}}}{\omega_{l,m}} \dot{c}_{l,m}(t) + 2V_{\mathrm{gen}}(t) \right). \tag{6}$$

Substituting (6) into (3) gives

$$\ddot{c}_{l,k}(t) + \omega_{l,k}^2 c_{l,k}(t) = \frac{i\omega_{l,k}}{\epsilon_0 \int_{\Omega_k} dV |\mathcal{E}_{l,k}(\boldsymbol{x}_k)|^2} \cdot \left\{ \begin{array}{l} \dfrac{V_{l,k\,\mathrm{loop}}^*}{Z_{\mathrm{gen}}} \left(2V_{\mathrm{gen}}(t) \right. \\ \left. + i \sum_{m=1}^{N} \dfrac{\dot{c}_{l,m}(t)}{\omega_{l,m}} V_{l,m\,\mathrm{loop}} \right) \\ - \int_{\Omega_k} dV \mathcal{E}_{l,k}^*(\boldsymbol{x}_k) \bullet \boldsymbol{J}_k(\boldsymbol{x}_k, t) \end{array} \right\}. \tag{7}$$

We now simplify (7) by assuming that all cavity drivers have a purely sinusoidal time-dependence, so that

$$V_{\rm gen}(t) = V_{\rm gen}e^{i\omega t} \tag{8}$$
$$\boldsymbol{J}_k(\boldsymbol{x}_k, t) = \boldsymbol{J}_k(\boldsymbol{x}_k)e^{i\omega t} \tag{9}$$
$$c_{l,k}(t) = c_{l,k}e^{i\omega t}. \tag{10}$$

To simplify the expressions for the cavity electric field define the bandwidth parameter

$$\Delta\omega_{l,k} = \frac{|V_{l,k\,\rm loop}|^2}{Z_{\rm gen}\epsilon_0 \displaystyle\int_{\Omega_k} dV|\mathcal{E}_{l,k}(\boldsymbol{x}_k)|^2} \tag{11}$$

and the frequency form factor function

$$f_{l,k}(\omega) = \frac{-i\omega\Delta\omega_{l,k}}{\omega^2 - i\Delta\omega_{l,k}\omega - \omega_{l,k}^2}. \tag{12}$$

The driven-cavity modal electric field is given by (not including the $e^{i\omega t}$ time dependence)

$$\boldsymbol{E}_{l,k}(\boldsymbol{x}_k) = c_{l,k}\frac{\omega}{\omega_{l,k}}\mathcal{E}_{l,k}(\boldsymbol{x}_k). \tag{13}$$

Equations (7)–(13) can be combined to express the driven-cavity modal electric field as

$$\boldsymbol{E}_{l,k}(\boldsymbol{x}_k) = f_{l,k}(\omega)\mathcal{E}_{l,k}(\boldsymbol{x}_k) \cdot \left\{ \frac{1}{V_{l,k\,\rm loop}}\left(2V_{\rm gen} - \omega\sum_{m\neq k}^{N}\frac{V_{l,m\,\rm loop}}{\omega_{l,m}}c_{l,m}\right) - \frac{Z_{\rm gen}}{|V_{l,k\,\rm loop}|^2}\int_{\Omega_k} dV\,\mathcal{E}^*_{l,k}(\boldsymbol{x}_k)\bullet\boldsymbol{J}_k(\boldsymbol{x}_k)\right\}. \tag{14}$$

For the case of a single (monoplet) cavity system with no electron beam current, the solution to (14) is trivial and the quantity $\Delta\omega_{l,k}$ is approximately equal to the bandwidth of the cavity. The next level of simplification is to assume that the buncher gap of each cavity is planar, so that the modal electric field within the beam is constant and can be represented by a gap voltage divided by a gap length. Additionally, it is assumed that the current density is not a function of r or θ in the buncher gap. For this approximation, $E_{z_{l,k}}(\boldsymbol{x}_k) = V_{l,k}/D_k$ and $\mathcal{E}_{z_{l,k}}(\boldsymbol{x}_k) = V_{l,k\,\rm gap}/D_k$, simplifying (14) to

$$V_{l,k} = f_{l,k}(\omega)\left\{G_{l,k}\left(2V_{\rm gen} - \sum_{m\neq k}^{N}\frac{V_{l,m}}{G_{l,m}}\right) - Z_{\rm gen}|G_{l,k}|^2\int_{\Omega_k} dV\frac{J_{z_k}(z_k)}{D_k}\right\}. \tag{15}$$

In examining (15), we can see that the only unknown variables in the equation are the $V_{l,k}$'s and $J_{z_k}(z_k)$. If $J_{z_k}(z_k)$ is determined, we have N equations in N unknowns and can solve for the $V_{l,k}$'s. In order to determine $J_{z_k}(z_k)$, we must self-consistently solve the electron-beam fluid equations in each buncher gap.

B. Fluid Equations for Buncher Gap

The 1-D fluid equations [4], [2] for a charged fluid with charge density, ρ, and flow velocity, u_z, are

$$J_z = \rho u_z \tag{16}$$
$$\frac{\partial\rho}{\partial t} + \rho\frac{\partial u_z}{\partial z} + u_z\frac{\partial\rho}{\partial z} = 0 \tag{17}$$
$$\frac{\partial u_z}{\partial t} + u_z\frac{\partial u_z}{\partial z} = \frac{e}{m}E_z. \tag{18}$$

We shall use a first-order time harmonic expansion of the dependent variables ignoring terms of order higher than $e^{i\omega t}$

$$\rho(z,t) = \rho^0(z)(1 + \tilde\rho(z)e^{i\omega t}) \tag{19}$$
$$u_z(z,t) = u_z^0(z)(1 + \tilde u(z)e^{i\omega t}) \tag{20}$$
$$J_z(z,t) = J_z^0(1 + \tilde J(z)e^{i\omega t}). \tag{21}$$

Substituting (19)–(21) into (16)–(18), we get

$$\tilde J(z) = \tilde\rho(z) + \tilde u(z) \tag{22}$$
$$\frac{d\tilde J}{dz} = -\frac{i\omega(\tilde J - \tilde u)}{u_z^0(z)} \tag{23}$$
$$\frac{d\tilde u}{dz} = \frac{e}{m}\frac{E_z}{(u_2^0)^2}e^{-i\omega t} - \frac{\tilde u}{u_z^0}\left(i\omega + 2\frac{du_z^0}{dz}\right). \tag{24}$$

Now make (22)–(24) specific to the kth buncher gap ($1 \le k \le N$) while defining the normalized variables (except for angles all dimensionless quatities are denoted by use of a tilde)

$$\tilde z_k = z_k/D_k \tag{25}$$
$$\tilde u_{z_k}^0(\tilde z_k) = u_{z_k}^0(\tilde z_k)/u_{z_k}^0(0) \tag{26}$$
$$\theta_k = \omega D_k/u_{z_k}^0(0) \tag{27}$$
$$\tilde Z_{\rm gen} = Z_{\rm gen}/Z_{\rm beam} \tag{28}$$
$$\tilde V_{\rm gen} = V_{\rm gen}/V_{\rm beam} \tag{29}$$
$$\tilde V_{l,k} = V_{l,k}/V_{\rm beam}. \tag{30}$$

In terms of these variables, (23) becomes

$$\frac{d\tilde J_k}{d\tilde z_k} = -i\frac{\theta_k}{\tilde u_{z_k}^0(\tilde z_k)}(\tilde J_k - \tilde u_k) \tag{31}$$

(24) becomes

$$\frac{d\tilde u_k}{d\tilde z_k} = \frac{\tilde V_{l,k}}{\tilde u_{z_k}^0(\tilde z_k)^2} - \frac{\tilde u_k}{\tilde u_{z_k}^0(\tilde z_k)}\left(i\theta_k + 2\frac{d\tilde u_{z_k}^0}{d\tilde z_k}\right) \tag{32}$$

and (15) becomes

$$\tilde V_{l,k} = f_{l,k}(\omega)\left\{G_{l,k}\left(2\tilde V_{\rm gen} - \sum_{m\neq k}^{N}\frac{\tilde V_{l,m}}{G_{l,m}}\right) - \tilde Z_{\rm gen}|G_{l,k}|^2\int_0^1 d\tilde z_k\tilde J_k\right\}. \tag{33}$$

Equations (31)–(33), with boundary conditions $\tilde u_1(0) = \tilde J_1(0) = 0$, make up the system that must be solved before we can determine the velocity modulation characteristics of

a multiplet buncher gap. First, consider what is included and what is not included in this system of equations. Beam loading is included through the current density integral in (33). RF space charge is not included, since only modal cavity fields are used to calculate the electric fields. Static space charge effects are included through the functions $\tilde{u}^0_{z_k}(\tilde{z}_k)$. These functions are the solutions to the electron fluid velocity function for each static (time-independent) planar gap in the system, and can be determined from the evaluation of the roots of a cubic equation [5]. The condition for ignoring space charge is $\tilde{u}^0_{z_k}(\tilde{z}_k) = 1$. Gap transit time effects are included through the parameter θ_k, which is the static (space charge fields are ignored) transit angle for an electron entering the kth buncher gap with velocity $u^0_{z_k}(0) = \sqrt{2eV_{\text{beam}}/m}$. We can solve this system iteratively by using a standard differential equation solver (Runge–Kutta) while varying the quantities $\int_0^1 d\tilde{z}_k \tilde{J}_k$ until a self-consistent solution is obtained. This procedure is currently under development. For the beam parameters and gaps currently of interest, I_{beam} is less than 5% of the gap's static limiting current and the analysis of the zero space charge case is sufficient for our needs. Please note that while the static space charge fields will be ignored in the following analysis, beam loading of the cavity is not ignored.

C. Zero Space Charge Approximation

For zero space charge ($\tilde{u}^0_{z_k}(\tilde{z}_k) = 1$), (31) and (32) of the multiplet cavity ($1 \le k \le N$) simplify to

$$\frac{d\tilde{J}_k}{d\tilde{z}_k} = -i\theta_k(\tilde{J}_k - \tilde{u}_k) \tag{34}$$

$$\frac{d\tilde{u}_k}{d\tilde{z}_k} = \tilde{V}_{l,k} - i\theta_k\tilde{u}_k. \tag{35}$$

Equation (33) is unchanged by the zero space charge condition. Equations (33)–(35) form a set of linear integro-differential equations with constant coefficients. Because the system has constant coefficients, a closed-form algebraic solution (solution of a linear algebraic system) can be constructed. First integrate (34) and (35) over each buncher gap to get

$$\tilde{J}_k(1) - \tilde{J}_k(0) = -i\theta_k\left(\int_0^1 d\tilde{z}_k\tilde{J}_k - \int_0^1 d\tilde{z}_k\tilde{u}_k\right) \tag{36}$$

$$\tilde{u}_k(1) - \tilde{u}_k(0) = \tilde{V}_{l,k} - i\theta_k\int_0^1 d\tilde{z}_k\tilde{u}_k. \tag{37}$$

Now solve (36) and (37) for $\int_0^1 d\tilde{z}_k\tilde{J}_k$ to get

$$\int_0^1 d\tilde{z}_k\tilde{J}_k = \frac{\tilde{V}_{l,k} + \tilde{J}_k(1) - \tilde{J}_k(0) + \tilde{u}_k(1) - \tilde{u}_k(0)}{i\theta_k}. \tag{38}$$

Equation (33) becomes

$$\tilde{V}_{l,k} = f_{l,k}(\omega)\left\{G_{l,k}\left(2\tilde{V}_{\text{gen}} - \sum_{m\neq k}^{N}\frac{\tilde{V}_{l,m}}{G_{l,m}}\right) - \frac{\tilde{Z}_{\text{gen}}|G_{l,k}|^2}{i\theta_k} \cdot (\tilde{V}_{l,k} + \tilde{J}_k(1) - \tilde{J}_k(0) + \tilde{u}_k(1) - \tilde{u}_k(0))\right\}. \tag{39}$$

To solve (34) and (35), use the standard formula for the solution of a first-order differential equation of the form $dy/dx + ay = F(x)$. The solution is $y(x) = e^{-ax}(\int_0^x dx' F(x')e^{ax'} + y(0))$. With this formula, the solution for (35) is

$$\tilde{u}_k(\tilde{z}_k) = \frac{1 - e^{-i\theta_k\tilde{z}_k}}{i\theta_k}\tilde{V}_{l,k} + \tilde{u}_k e^{-i\theta_k\tilde{z}_k}. \tag{40}$$

Substituting (40) into (34) gives

$$\frac{d\tilde{J}_k}{d\tilde{z}_k} + i\theta_k\tilde{J}_k = (1 - e^{-i\theta_k\tilde{z}_k})\tilde{V}_{l,k} + i\theta_k\tilde{u}_k(0)e^{-i\theta_k\tilde{z}_k}. \tag{41}$$

Using the standard solution formula again produces the solution to (41) for $\tilde{z}_k = 1$

$$\tilde{J}_k(1) = (i\theta_k\tilde{u}_k(0) + \tilde{J}_k(0))e^{-i\theta_k} + \left(\frac{1 - e^{-i\theta_k}}{i\theta_k} - e^{-i\theta_k}\right)\tilde{V}_{l,k}. \tag{42}$$

If we define the following coefficients:

$$a_k = e^{-i\theta_k} \tag{43}$$

$$b_k = i\theta_k e^{-i\theta_k} \tag{44}$$

$$c_k = \frac{1 - e^{-i\theta_k}}{i\theta_k} \tag{45}$$

$$d_k = \frac{1 - e^{-i\theta_k}}{i\theta_k} - e^{-i\theta_k} \tag{46}$$

$$e_{l,k} = f_{l,k}(\omega)G_{l,k} \tag{47}$$

$$g_{l,k} = -f_{l,k}(\omega)\frac{\tilde{Z}_{\text{gen}}|G_{l,k}|^2}{i\theta_k} \tag{48}$$

the equations describing the multiplet buncher become

$$\tilde{u}_k(1) - a_k\tilde{u}_k(0) - c_k\tilde{V}_{l,k} = 0 \tag{49}$$

$$\tilde{J}_k(1) - b_k\tilde{u}_k(0) - a_k\tilde{J}_k(0) - d_k\tilde{V}_{l,k} = 0 \tag{50}$$

$$(1 - g_{l,k})\tilde{V}_{l,k} + e_{l,k}\sum_{m\neq k}^{N}\frac{\tilde{V}_{l,m}}{G_{l,m}} + g_{l,k}(\tilde{J}_k(1) - \tilde{J}_k(0) + \tilde{u}_k(1) - \tilde{u}_k(0)) = 2e_{l,k}\tilde{V}_{\text{gen}}. \tag{51}$$

For the specific case of the multiplet cavity, the output of the $k-1$ cavity is the input to cavity k. This condition generates the additional boundary conditions

$$\tilde{u}_k(0) = \tilde{u}_{k-1}(1) \tag{52}$$

$$\tilde{J}_k(0) = \tilde{J}_{k-1}(1). \tag{53}$$

Define the variables (not functions of $\tilde{z}_k$) $\tilde{u}_k$ and $\tilde{J}_k$ for $0 \le k \le N$

$$\tilde{u}_k = \begin{Bmatrix}\tilde{u}_k(1) & 1 \le k \le N \\ \tilde{u}_1(0) & k = 0\end{Bmatrix} \tag{54}$$

$$\tilde{J}_k = \begin{Bmatrix}\tilde{J}_k(1) & 1 \le k \le N \\ \tilde{J}_1(0) & k = 0\end{Bmatrix}. \tag{55}$$

Substitute (54) and (55) into (49)–(51) to get

$$\tilde{u}_k - a_k\tilde{u}_{k-1} - c_k\tilde{V}_{l,k} = 0 \tag{56}$$

$$\tilde{J}_k - b_k\tilde{u}_{k-1} - a_k\tilde{J}_{k-1} - d_k\tilde{V}_{l,k} = 0 \tag{57}$$

$$(1-g_{l,k})\tilde{V}_{l,k}+e_{l,k}\sum_{m\neq k}^{N}\frac{\tilde{V}_{l,m}}{G_{l,m}}$$
$$+\,g_{l,k}(\tilde{u}_k-\tilde{u}_{k-1}+\tilde{J}_k-\tilde{J}_{k-1})=2e_{l,k}\tilde{V}_{\rm gen}. \quad (58)$$

When the initial conditions for the buncher cavity ($\tilde{u}_0=0$ and $\tilde{J}_0=0$) are imposed, (56)–(58) become a linear system of $3N$ equations in $3N$ variables and can be solved with a standard linear algebra subroutine package. We will now examine the implications of the performance of such a system, where $N=2$ (doublet buncher).

III. Doublet Cavity Studies

A. Implementation of Multiplet Analysis

A C++ program has been written that takes as input all relevant multiplet buncher cavity parameters, and then calculates the coefficient matrices for (49)–(51), solves the linear system of equations, and plots the velocity modulation at the output of each cavity of the multiplet and the ballistic focusing distance (60) for the beam emerging from the Nth cavity of the multiplet. For $N=2$, these operations take less than one second to evaluate the multiplet response at 500 different frequencies (50-MHz 486 PC running under the Linux operating system). All the code is in the public domain (including the X-window plotting package VOGLE and the linear algebra class libraries) and is available from the author on request.

B. Klystron Definition

The klystron characteristics common to all configurations currently under investigation are shown in Table I. The two unusual characteristics (compared to conventional klystrons) are the beam perveance, which is much higher than in a conventional klystron, and the impedance of the RF driver, which is much lower than the typical value of 50 Ω. The treatment of the transport of a high-perveance beam in the drift regions of the klystron is outside the scope of this paper. (As an example, one might conceive of a multibeam configuration in the drift region, where the beamlets are transported in an array of isolated tubes, which drastically reduces the space charge fields, and allows for simple ballistic focusing.) The low RF generator impedance can easily be achieved by having parallel drive loops, equispaced around the circumference of the cavity, driven by an array of solid-state amplifiers. The high-perveance beam is required for the design of a broad-band output cavity. The low-impedance driver generator is required for a broad-band buncher cavity.

Consider (11), but rewrite the modal drive loop voltage in terms of the modal gap voltage, $V_{l,k\,\rm gap}$, and the gap gain, $G_{l,k}$, to get

$$\frac{\Delta\omega_{l,k}}{c}=\frac{Z_0|V_{l,k\,\rm gap}|^2}{Z_{\rm gen}\displaystyle\int_{\Omega_k}dV|\mathcal{E}_{l,k}(\boldsymbol{x}_k)|^2}\frac{1}{|G_{l,k}|^2}. \quad (59)$$

TABLE I
Klystron Parameters

P_{beam}	20	kW
$\wp_{beam}$	10	μperv
V_{beam}	5.25	kV
I_{beam}	3.8	A
R_{beam}	0.78	cm
R_{drift}	1	cm
Z_{gen}	12.5	Ω
f_0	1	GHz

The quantity $\Delta\omega_{l,k}$ is, to first order, half the bandwidth of the kth cavity of the multiplet, not including the effects of beam loading. In order to design a broad-band buncher cavity, $\Delta\omega_{l,k}$ must be comparable to the required system bandwidth divided by the order, N, of the multiplet cavity. If we wish to keep the order of the multiplet cavity to a reasonable value, say $N=2$, then $\Delta\omega_{l,k}$ must be about half the required system bandwidth. The two parameters of (59) that we can exercise some reasonable control over are the generator impedance, $Z_{\rm gen}$, and the gap gain, $G_{l,k}$. The other terms in (59) depend purely upon the distribution of the cavity electric field eigenmode, and hence depend only upon the cavity dimensions. (It would help to keep the impedance of the transmission-line section of the resonator as high as practical to reduce the energy stored in the electric field.) In contrast, $Z_{\rm gen}$ can be reduced by the use of parallel phase-locked RF drive generators, and $G_{l,k}$ can be adjusted by placement of the drive loop in the cavity.

Before calculating the buncher cavity response for specific cases, we must consider what is meant by a broad-band buncher cavity. One extreme answer would be a buncher with a flat (<1 dB) velocity modulation response over a wide range of drive frequencies. Another extreme answer would be a buncher that produces a flat (<1 dB) focusing distance response over a wide range of frequencies. The ballistic focusing distance (ignoring space–charge effects) in a drift region is given by

$$z_{\rm focus}=\frac{\sqrt{2eV_{\rm beam}/m}}{\omega|\tilde{u}_N|}. \quad (60)$$

Since $z_{\rm focus}$ is proportional to $1/\omega$, the buncher parameters that produce a flat focusing response will be very different from those that produce a flat velocity-modulation response. In reality, space–charge effects will modify the relationships among focusing distance, frequency, and velocity modulation amplitude to produce a result intermediate between simple ballistic focusing (60), and one where constant velocity modulation as a function of frequency is required. Thus, if we can

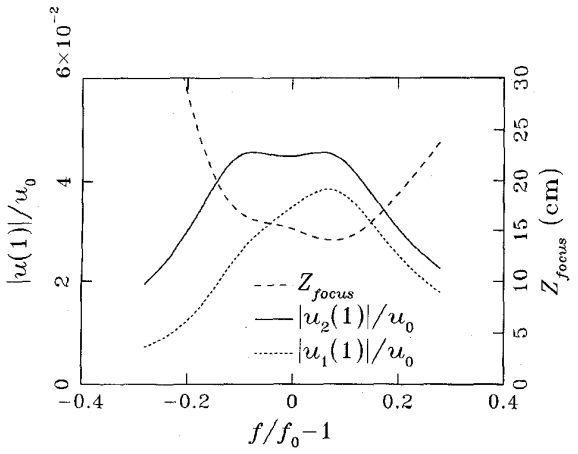

$P_{gen} = 20$ W

k	1	2	
$f_{l,k}$	1.15	0.85	GHz
$G_{l,k}$	3.05	2.93	
D_k	0.34	0.34	cm
L_k	6.0	7.9	cm
R_{max_k}	1.40	1.95	cm

Fig. 3. Ten-kilowatt doublet buncher cavity with 20% velocity modulation bandwidth.

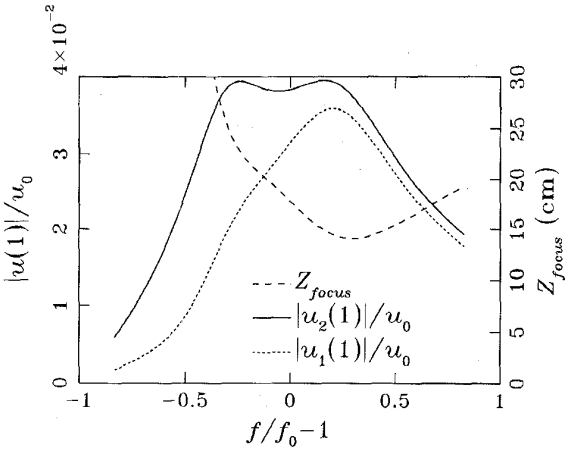

$P_{gen} = 50$ W

k	1	2	
$f_{l,k}$	1.42	0.63	GHz
$G_{l,k}$	1.93	1.80	
D_k	0.34	0.34	cm
L_k	4.8	11.0	cm
R_{max_k}	1.40	1.95	cm

Fig. 4. Ten-kilowatt doublet buncher cavity with 50% velocity modulation bandwidth.

demonstrate that the doublet buncher cavity can be designed to produce a flat response for the two extreme cases, it should be possible to design the cavity to provide a flat response to a focusing function that includes space–charge effects.

The method we employ to optimize a doublet buncher cavity is to program a solution to the system defined by (56)–(58), and to plot the magnitude of the velocity modulation at the outputs of cavity 1 and cavity 2. In addition, the modulation amplitude at the output of cavity 2 is used to calculate a ballistic focusing distance from (60), which is also plotted. The parameters that are varied to optimize the buncher cavity are the resonant frequency and gap gain of each cavity. The procedure is not automated, but iterated interactively.

C. Optimization of Velocity Modulation

In the first example, the system is specified to have a velocity modulation bandwidth of 20%. We begin the design process by choosing a reasonable driver generator power of 20 W. Then $G_{l,k}$ is chosen so that $\Delta\omega_{l,k}/\omega_{l,k} \approx 0.1$, and the system is interactively iterated by varying the center frequencies and gap gains of each cavity until the plotted output indicates that the velocity modulation bandwidth is approximately 20%. The result of several iterations is shown in Fig. 3. Fig. 3 plots the normalized velocity modulation at the output of each gap (see annotations on Fig. 3) and z_{focus}, the axial position of maximum beam bunching, as a function of normalized frequency, $f/f_0 - 1$.

One critical element of Fig. 3 is that the separation of the resonant frequencies of the cavities (in this case 0.3 GHz) is significantly greater than the separation of the peaks of the velocity modulation curve (in this case <0.2 GHz). The

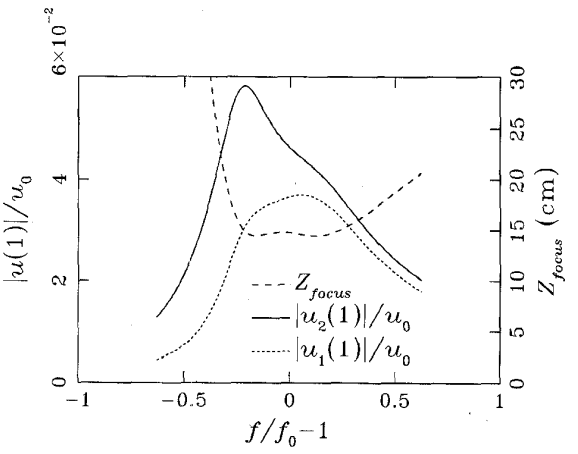

$P_{gen} = 50$ W

k	1	2	
$f_{l,k}$	1.27	0.70	GHz
$G_{l,k}$	2.02	2.25	
D_k	0.34	0.34	cm
L_k	5.4	9.8	cm
R_{max_k}	1.40	1.95	cm

Fig. 5. Ten-kilowatt doublet buncher cavity with 50% focusing distance bandwidth.

reason for this is that the first (high-frequency) cavity is generating significant velocity modulation at the entrance of the second (low-frequency) cavity, at frequencies above the resonant frequency of the second cavity. The premodulation in this frequency range (see $|\tilde{u}_1(0)|$ in Fig. 3) significantly

enhances the second cavity's ability to velocity modulate the electron beam. These effects in the two cavities are much more than additive. The next design goal is to increase the velocity modulation bandwidth to 50%. To do this we can decrease the gap gains to increase the bandwidth of each cavity, increase the separation of the resonant frequencies of the two cavities, and increase the drive generator power to regain velocity modulation amplitude lost though decreasing the gap gains. The results of the new design after several iterations are shown in Fig. 4. In the new design, the resonance separation has increased to 0.79 GHz, and the average gap gain has decreased to 1.9. The velocity modulation bandwidth of the new design is at least 50%.

D. Optimization of Ballistic Focusing Distance

As a final buncher cavity design exercise, we can take the design from Fig. 4 and modify it so that z_{focus} as a function of frequency is flat. The method used is to increase the gap gain of the low-frequency cavity until the focusing length in the low-frequency region is approximately equal to its minimum value in the high-frequency region. Then the cavity resonance separation is changed to reduce any peaks in the focusing response at frequencies between these regions. The result of iterating this process several times is shown in Fig. 5. In the modified design, the resonance separation has decreased to 0.57 GHz, and the average gap gain has increased to 2.17. The focusing distance bandwidth of the modified design is at least 50%. The focusing distance over the bandwidth of this design is 15 cm. This length is quite reasonable for the drift length of a 1-GHz klystron.

IV. Conclusions

We have shown, in the planar gap approximation and for a high-perveance multikilowatt electron beam, that using a doublet buncher cavity allows us to realize a 50% bandwidth cavity, either in velocity modulation or focusing distance. A simple computer code allows an interactive iterative method of designing such buncher cavities. Additionally, the ballistic focusing distances for the beams emerging from such cavities are of modest length and could lead to the construction of compact high-power klystron amplifiers.

Acknowledgment

The author wishes to thank H. E. Brandt and D. K. Abe for helpful discussions throughout the course of this research.

References

[1] R. S. Symons, Litton Electron Devices Division, private communication.
[2] A. Bromborsky, "Analysis and simulation of broadband klystron amplifiers," ARL Tech. Rep., in preparation.
[3] R. S. Symons and J. R. M. Vaughan, "The linear theory of the clustered-cavity^{TM} klystron," *IEEE Trans. Plasma Sci.*, vol. 22, no. 5, pp. 713–718, 1994.
[4] D. C. Montgomery and D. A. Tidman, *Plasma Kinetic Theory*. New York: McGraw-Hill, 1964, p. 118.
[5] C. K. Birdsall and W. B. Bridges, *Electron Dynamics of Diode Regions*. New York: Academic, 1966, pp. 69–72.

Alan Bromborsky (S'67–M'68), for a photograph and biography, see this issue, p. 851.